NUMMERICAL AND SIMULATION METHODS FOR CALCULATION OF DYNAMICAL TRANSIENT CHARACTERISTICS OF SQUIRREL CAGE INDUCTION MOTOR

ЦИФРОВИ И СИМУЛАЦИОННИ МЕТОДИ ЗА ПРЕСМЯТАНЕ НА ДИНАМИЧНИТЕ ПРЕХОДНИ ХАРАКТЕРИСТИКИ НА АСИНХРОНЕН ДВИГАТЕЛ С НАКЪСО СЪЕДИНЕН РОТОР

Assist. prof. Dr. Eng. Sarac V.[1], Assistant Msc. Eng. Stefaov G. [2]
Electrotechnical Faculty – University 'Goce Delcev'-Stip, Macedonia [1,2]

Abstract: *In this paper induction squirrel cage motor is analyzed with respect to its dynamical behaviour. First analytical calculation of motor's parameters and characteristics is performed by developing software program for their calculation. MATLAB is used for calculation of system of five differential equations with constant coefficients with Runge Kutta method of fourth order resulting in transient motor characteristics of speed and electromagnetic torque at different operational regimes. Transient characteristics are obtained as well as from simulation model developed in SIMULINK. Characteristics from both transient models are compared and conclusions are derived with respect to available data from experimental measurements and from manufacturer side.*
Keywords: INDUCTION MOTOR, TRANSIENT CHARACTERISTICS, NUMERICAL MODEL, SIMULATION MODEL

1. Introduction

Squirrel cage induction motor has wide application in many industrial drive systems due to its simple construction, robust design and operational behaviour. Its application becomes even wider due to voltage inverters which enable very good speed-torque regulation characteristics. In this paper squirrel cage induction motor type 2AZ 155-4 from producer Rade Koncar is analyzed with respect to its dynamic behaviour. Motor has following rated data: voltage Un (Y/Δ)=220/380 V, number of poles 2p=4, rated current 8,7/5 A, power factor cosφ=0,81, rated speed n_n=1410 rpm, frequency 50 Hz. Motor cross section is presented on Fig.1

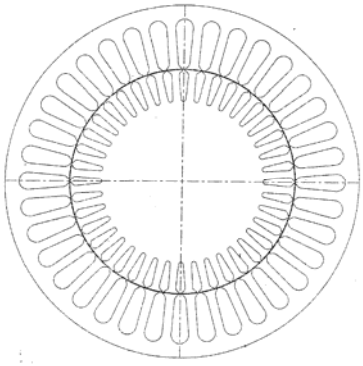

Fig.1 Motor's cross section

Motor's parameters and characteristics using analytical approach are calculated by developing a program in FORTRAN. On the base of obtained results motor operation characteristics are plotted, as well as no-load characteristics and electromagnetic characteristic. Motor's dynamic behaviour is described with system of five linear differential equations with constant coefficients. Solution of this systems with numerical Runge Kutta method of IV order in MATLAB leads to transient characteristics of speed and electromagnetic torque versus time. Accuracy of these characteristics is confirmed by comparison with transient characteristics obtained from simulation model developed in SIMULINK. Results from both models are compared with available data from manufacturer and from experimental measurements.

2. Development of analytical model

On the base of the software calculation in FORTRAN motor operational characteristics are calculated : stator current-I_1, efficiency factor-η, power factor-cosφ, input power-P_1, speed-n and output torque M_2 versus output power: $I_1=f(P_2)$, $\eta=f(P_2)$, $\cos\varphi=(P_2)$, $P_1=f(P_2)$, $n=f(P_2)$, and $M_2=f(P_2)$. Mechanical characteristic of electromagnetic torque M_{em} for different motor slips-s is calculated from motor T-equivalent circuit.

Operational characteristics are plotted on the base of results given in Table 1.

Table 1. Motor operational characteristics

I_1 [A]	η [%]	cosφ [/]	s p.u.	P_1 [W]	n [rpm]	M_2 [Nm]	P_2 [W]
2.17	0.128	0.119	0.00062	171.32	1499.07	0.21	22
2.22	0.59	0.255	0.00433	372.62	1493.5	1.48	220
2.32	0.73	0.392	0.00858	600.87	1487.13	2.9	440
2.49	0.79	0.508	0.01298	834.26	1480.53	4.34	660
2.71	0.82	0.601	0.01754	1073.14	1473.69	5.79	880
2.97	0.835	0.673	0.0223	1317.98	1466.56	7.25	1100
3.27	0.841	0.727	0.02727	1569.3	1459.1	8.73	1320
3.60	0.843	0.768	0.0325	1827.73	1451.26	10.23	1540
3.97	0.84	0.799	0.03802	2094.09	1442.97	11.74	1760
4.37	0.836	0.822	0.4389	2369.36	1434.16	13.28	1980
4.79	0.83	0.838	0.05019	2654.83	1424.72	14.85	2200

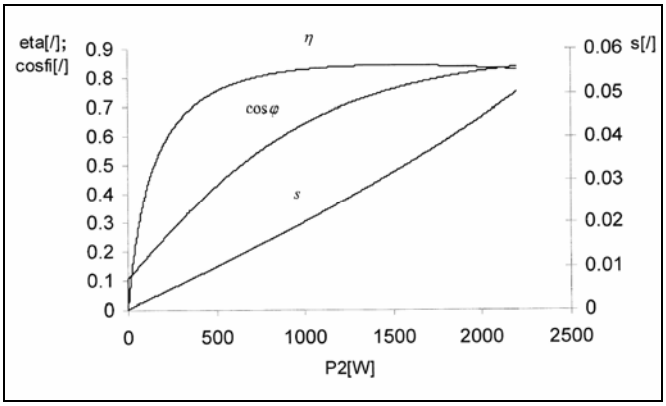

Fig.2 Operational characteristics $\eta=f(P_2)$, $\cos\varphi=f(P_2)$, $s=f(P_2)$

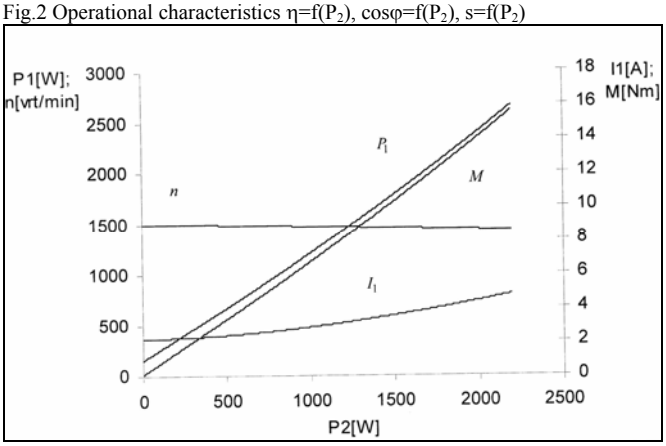

Fig.3 Operational characteristics $n=f(P2)$, $M_2=f(P2)$, $I_1=f(P_2)$

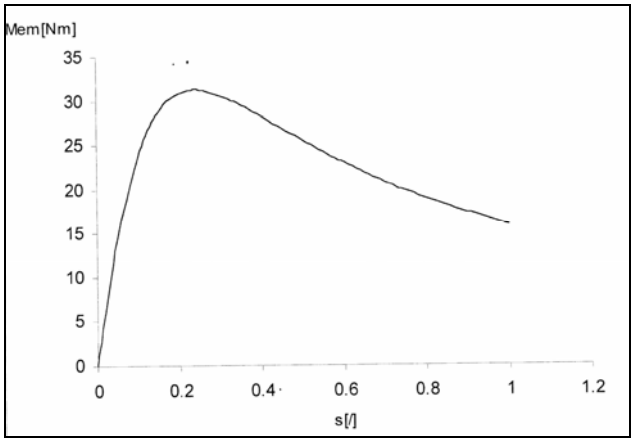

Fig.4 Mechanical characteristic $M_{em}=f(s)$

3. Development of numerical model

System of n-differential equation of first order is represented by:

$$(1)\quad \begin{aligned} \frac{dy_1(x)}{dx} &= f_1(x, y_1, y_2, ...y_n) \\ \frac{dy_2(x)}{dx} &= f_2(x, y_1, y_2, ...y_n) \\ &..... \\ \frac{dy_n(x)}{dx} &= f_n(x, y_1 y_2, ...y_n) \end{aligned}$$

It can be solved by different numerical methods: Euller, Bulirsch-Stoer, Runge Kutta etc. Application of appropriate method is determined by boundary conditions and starting conditions which must be defined in order system of equations to be solvable. When it is used Euller method values of the function y_i are determined for starting condition $x=x_p$. Increasment of Δx leads to changes in all functions y_i for adequate increasments Δy_i.

$$(2)\quad y_i(x_p+\Delta x) \approx y_i(x_p)+\Delta y_i$$

Equation (2) can be adequately replaced with:

$$(3)\quad \Delta y \cong f_i(x, y_1, y_2, ..., y_n)\Delta x$$

From equation (2) and (3) values of the function y_i in new point $x_p+\Delta x_p$ are known. By applying the same procedure value of the function $y_i(x_p+2\Delta x)$ can be achieved. Consequently step by step value of the function y_i in final point $x=x_k$ can be calculated. This is an Euller method which does not give an adequate accuracy. For practical calculation and for more accurate results Runge Kutta method with adaptive step is used.

If system (1) is solved with Euller method for step Δx from point x up to point $x+\Delta x$ following solution is obtained:

$$(4)\quad y_i(x+\Delta x) = y_i(x)+ f(x, y_i, ..., y_n)\Delta x + error$$

If this error is from order $(\Delta x)^2$ method is from first order. A Euller method uses information about derivations from the beginning of the interval $(x, x+\Delta x)$ for extrapolation of the starting values of y_i on the end of the interval. As a result accuracy of the method is low. It is better to be used values of the derivation from the beginning, middle and end of the interval $(x, x+\Delta x)$. On the base of these values better estimation of the value y_i $(x+\Delta x)$ on the end of the interval is obtained. This is the base for the whole family of Runge Kutta methods. Most frequently used is Runge Kutta of forth or fifth order where error is proportional with $(\Delta x)^5$, i.e. $(\Delta x)^6$.

Motor dynamic transient operational regime is determined by following system of linear differential equations:

$$(5)\quad \begin{aligned} \frac{d\psi_{s\alpha}}{dt} &= \sqrt{2}U_n \cos\omega t - a_1\psi_{s\alpha} + a_2\psi_{r\alpha} \\ \frac{d\psi_{s\beta}}{dt} &= \sqrt{2}U_n \sin\omega t - a_1\psi_{s\beta} + a_2\psi_{r\beta} \\ \frac{d\psi_{r\alpha}}{dt} &= a_3\psi_{s\alpha} - a_4\psi_{r\alpha} - \omega_r\psi_{r\beta} \\ \frac{d\psi_{r\beta}}{dt} &= a_3\psi_{s\beta} - a_4\psi_{r\beta} + \omega_r\psi_{r\alpha} \\ \frac{d\omega_r}{dt} &= p(M_{em} - M_s)/J \\ M_{em} &= a_5(\psi_{s\beta}\psi_{r\alpha} - \psi_{r\beta}\psi_{s\alpha}) \end{aligned}$$

where ω=314 [rad/s], J is motor moment of inertia and a_1, a_2, a_3, a_4 and a_5 are coefficient which are determined by motor parameters stator and rotor resistance R_s and R_r stator and rotor inductance L_s and L_r and mutual inductance L_m:

$$a_1 = \frac{R_s L_r}{L_s L_r - L_m} \quad a_2 = \frac{R_s L_m}{L_s L_r - L_m^2} \quad a_3 = \frac{R_r L_s}{L_s L_r - L_m^2}$$

$$a_4 = \frac{R_r L_m}{L_s L_r - L_m^2} \quad a_5 = \frac{1{,}5\, p L_m}{L_s L_r - L_m^2}$$

Equation (5) gives the system of five differential equations with five unknown variables. They describe the motor stator and rotor circuit while the six equation calculates the electromagnetic torque on the base fluxes in stator and rotor circuits which are described with $\psi_{s\alpha}, \psi_{s\beta}, \psi_{r\alpha}$ and $\psi_{r\beta}$ respectively. Solution of systems of equation (5) gives the transient characteristics of electromagnetic torque M_{em} [Nm] and rotor angular speed ω_r [rad/s] when motor is supplied with three phase symmetrical power supply.

3. Development of simulation model

Simulation of motor transient characteristics in SIMULINK is performed by building a simulation model. On Fig. 5 is presented a block diagram of simulation model consisted of following four main parts [1]:

- Power supply
- Transformation of a,b,c variables into variables in d,q system which rotates synchronously.
- Modelling of motor model and obtaining motor speed and electromagnetic torque as output variables.
- Transformation from d,q system into a,b,c system in order stator and rotor voltages and currents to be obtained.

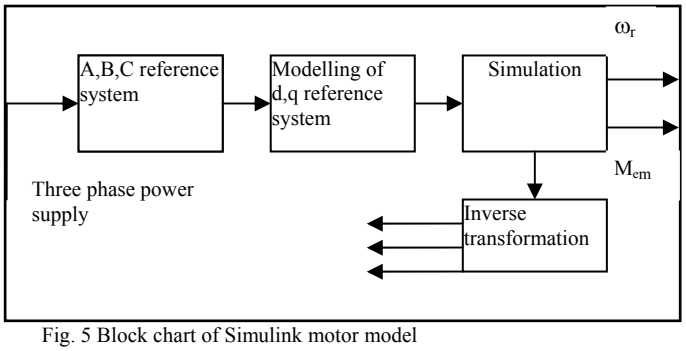

Fig. 5 Block chart of Simulink motor model

First motor power supply (three phase symmetrical power supply) is transformed from three phase system into d,q system which rotates with synchronous speed [2] as it is presented with equations (6) and (7).

(6) $U_{ds} = -\frac{1}{\sqrt{3}}(U_b - U_c)\cos\theta + U_a \sin\theta$

(7) $U_{qs} = \frac{1}{\sqrt{3}}(U_b - U_c)\sin\theta + U_a \cos\theta$

where : $\omega = \frac{d\theta}{dt}$ i.e. $\theta = \int_0^t \omega dt$

Since power supply is three phase symmetrical power supply in that case $\omega = \omega_e = 314[rad/s]$. Simulation model is based on following equations:

$$i_{qr} = \frac{L_s R_r}{L_m^2 - L_s L_r}\int_0^t i_{qr}dt + \frac{\omega L_s L_r}{L_m^2 - L_s L_r}\int_0^t i_{dr}dt +$$

$$(8)\ \frac{L_{sr}\omega}{L_m^2 - L_s L_r}\int_0^t \psi_{ds}dt + + \frac{L_{sr}^2 - L_s L_r}{L_m^2 - L_s L_r}\int_0^t \omega_r i_{dr}dt -$$

$$\frac{L_{sr}}{L_m^2 - L_s L_r}\int_0^t \omega_r \psi_{ds}dt + \frac{L_{sr}}{L_m^2 - L_s L_r}\psi_{qs}$$

$$i_{qr} = \frac{L_s R_r}{L_m^2 - L_s L_r}\int_0^t i_{dr}dt - \frac{\omega\left(L_{sr}^2 - L_s L_r\right)}{L_m^2 - L_s L_r}\int_0^t i_{qr}dt -$$

$$(9) - \frac{L_{sr}\omega}{L_m^2 - L_s L_r}\int_0^t \psi_{qs}dt - \frac{L_{sr}^2 - L_s L_r}{L_m^2 - L_s L_r}\int_0^t \omega_r i_{qr}dt$$

$$+ \frac{L_{sr}}{L_m^2 - L_s L_r}\int_0^t \omega_r \psi_{qs}dt + \frac{L_{sr}}{L_m^2 - L_s L_r}\psi_{ds}$$

In the equations (8) and (9) flux leakages are unknown variables and they can be expressed from:

(10) $\psi_{qs} = \int_0^t U_{qs}dt - \frac{R_s}{L_s}\int_0^t \psi_{qs}dt + \frac{L_{sr}R_s}{L_s}\int_0^t i_{qr}dt - \omega\int_0^t \psi_{ds}dt$

(11) $\psi_{ds} = \int_0^t U_{ds}dt - \frac{R_s}{L_s}\int_0^t \psi_{ds}dt + \frac{L_{sr}R_s}{L_s}\int_0^t i_{dr}dt + \omega\int_0^t \psi_{qs}dt$

Motor speed is calculated from:

(12) $\frac{d\omega_r}{dt} = \frac{6L_{sr}}{J}\left(i_{qs}i_{dr} - i_{ds}i_{qr}\right) - \frac{2}{J}M_s - \frac{2}{J}M_0$

where M_s is load torque, M_0 is a torque as a result of acceleration at no-load.

4. Comparison of results

In this section comparison between transient characteristics obtained from numerical and simulation model will be presented. On Fig.6 and 7 are presented transient characteristics of speed and electromagnetic torque at no-load acceleration.

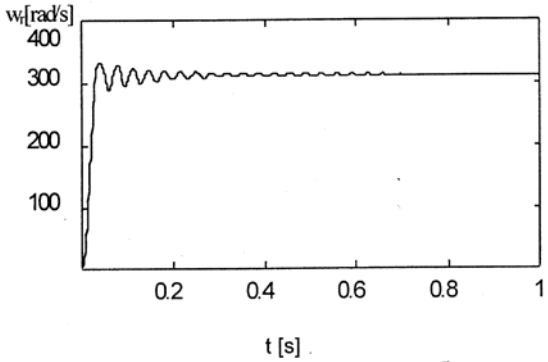

(a)

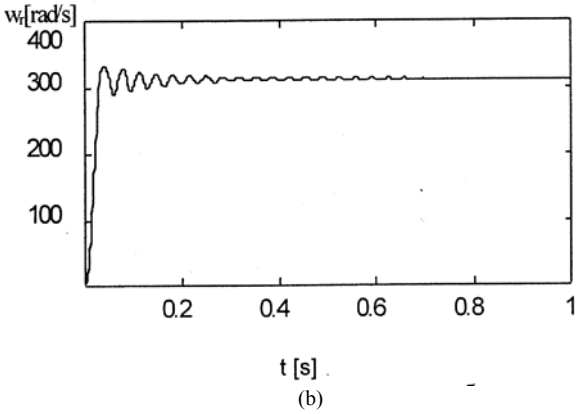

(b)

Fig. 6 Transient characteristics of speed at no load (a) simulation model (b) numerical model

From Fig.6 can be concluded that motor acceleration by both methods is ended in approximately same time interval of 0,025 s. Transient characteristic $\omega_r = f(t)$ from numerical model has more oscillations after motor acceleration is finished. In both motor models same speed at no-load operation condition is achieved of 313[rad/s].

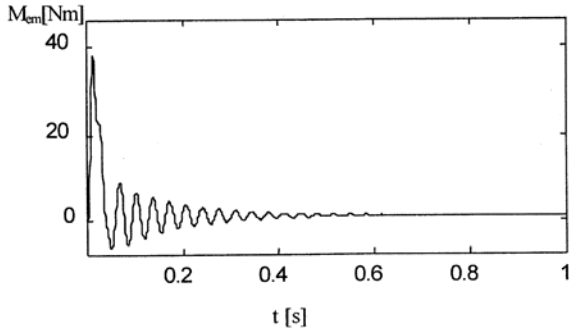

(a)

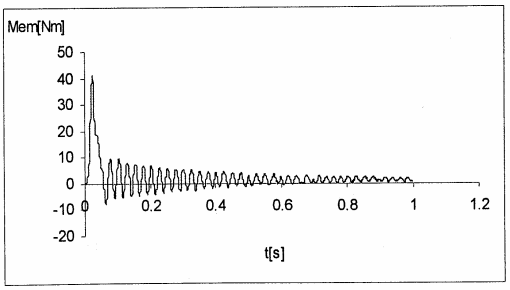

(b)

Fig. 7 Transient characteristics of electromagnetic torque at no load (a) simulation model (b) numerical model

From Fig.7 can be concluded that in both models after motor acceleration is finished for acc. 0,025 s , electromagnetic torque drops up to value of 1.1 Nm i.e. up to the value of no-load torque.

On Fig. 8 and 9 are presented transient characteristics of speed and electromagnetic torque at rated load condition Ms=14 Nm.

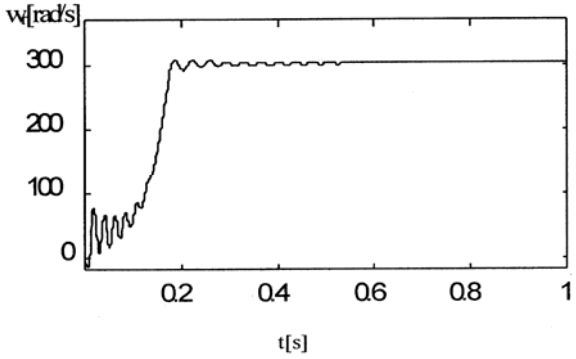

(a)

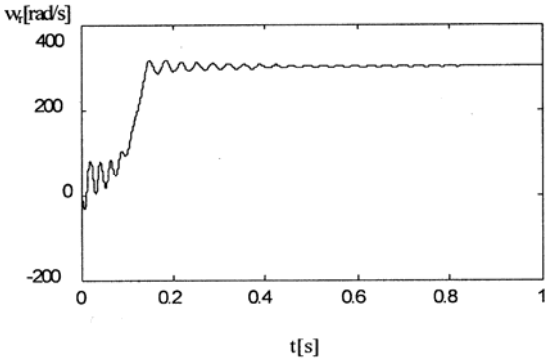

(b)

Fig. 8 Transient characteristics of speed at Ms=14Nm
(a) simulation model (b) numerical model

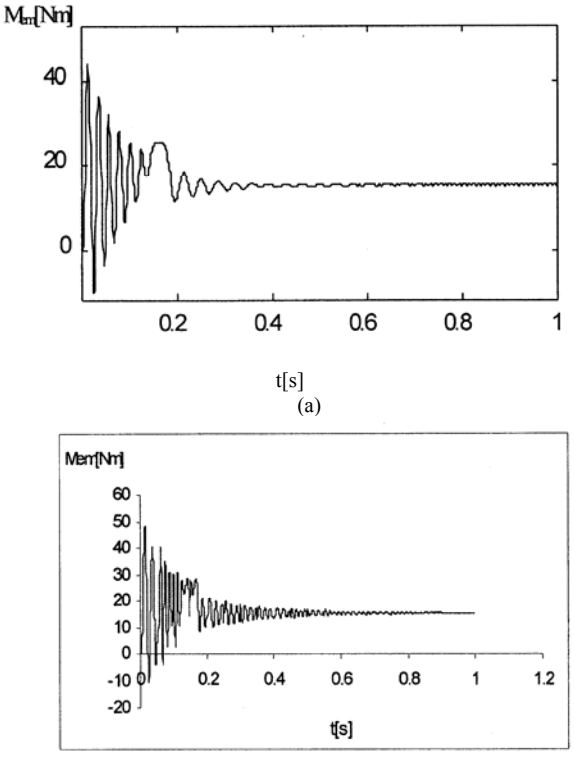

(a)

(b)

Fig. 9 Transient characteristics of electromagnetic torque at Ms=14Nm
(a) simulation model (b) numerical model

In Table 2 are presented results of different slips for different electromagnetic torques obtained by analytical model and simulation.

Table 2. Motor slip from analytic calculation and simulation

	Analytic	Simulation
M_{em} [Nm]	s[/]	s [/]
1	0.0036	0.0067
2	0.007	0.008
3	0.0105	0.01
4	0.0138	0.013
5	0.017	0.0167
6	0.0198	0.021
7	0.0232	0.024
8	0.0265	0.026
9	0.0301	0.0277
10	0.0332	0.031
11	0.0373	0.034
12	0.0406	0.036
13	0.0446	0.041
14	0.0485	0.043

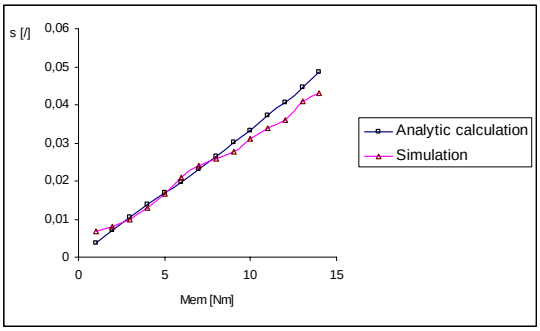

Fig. 10 Comparison of motor slip from analytical and simulation model

From Fig.8 can be concluded that in numerical model motor acceleration is going faster approximately in 0,14 s while in Simulink model it rates up to 0,18 s. In both cases motor accelerates up to 300 [rad/s]. From Fig. 9 it is noticeable the similarity between both transient characteristics $M_{em}=f(t)$ obtained by both motor models. In both cases after acceleration electromagnetic torque decreases up to the value of 15,2 Nm.

In Table 3 comparatively are presented results obtained by different methods.

	Producer	Analytical calculation	Experim.	Sim. model	Num. model
P_n[W]	2200	2200	2200		
n_n [rpm]	1410	1424,72	1410	1427,2	1430
I_n [A]	5	4,8	4,87	4,5	/
s_n[/]	0,06	0,058	0,06	0,053	0,051
cosφ[/]	0,81	0,838	0,78	/	/
η [/]	/	0,828	0,79	/	/
M_n [Nm]	14,9	14,67	13,8		
$M_{em\ n}$[Nm]	16	16,58	13,88	15,2	15

5. Conclusion

Complex analysis of operational and transient characteristics of squirrel cage induction motor is performed. For that purpose three motor models are developed: analytical, numerical and simulation model. While the analytical model is mainly used for calculation of motor operational characteristics and mechanical characteristics, numerical and simulation models are used for calculation of transient dynamic characteristics of speed and electromagnetic torque versus time. At no load operating regime motor accelerates up to 313 [rad/s] for approximately the same time of 0,025 s in both models. After acceleration electromagnetic torque decreases up to 1,1 Nm. At rated load operating regime motor accelerates up to 300[rad/s] for 0,18s in simulation model and for 0,14s in numerical model. From the producer data rated speed is 295 [rad/s]. Agreement of the simulation results with producer data is satisfactory. After acceleration electromagnetic torque decrease up to the value of 15,2 Nm in both motor models, which is expected result considering producer data for rated electromagnetic torque of 16 Nm. From presented transient characteristics it is obvious the similarity of obtained results which confirms the accuracy of both models. Oscillations in transient characteristics are larger for the numerical model due to the strict conditions for stability of mathematical solution in numerical methods.

6. References

[1] V.Sarac, L.Petkovska, M. Cundev: 'Transient performance characteristics of inverter fed induction motor', 10-th EDPE-Electrical Drives and Power Electronic Conference, 14-16.X.1998.

[2] Krause, O. Wasynczuk, S.D. Sudhoff: 'Analysis of electrical machinery', IEEE Press , 2nd Edition, New York, USA 1995.